J Polym Res (2015) 22: 57
DOI 10.1007/s10965-015-0703-9

ORIGINAL PAPER

Open-cell macroporous bead: a novel polymeric support for heterogeneous photocatalytic reactions

Yun Zhu[1] · **Ye Hua**[1] · **Shengmiao Zhang**[1] · **Yanhua Wang**[1] · **Jianding Chen**[1]

Received: 12 November 2014 / Accepted: 13 March 2015 / Published online: 21 March 2015

Abstract A novel polymeric support for heterogeneous photocatalytic reactions was fabricated by using a multiple O/W/O emulsion as the template, which was an open-cell macroporous bead with photocatalyst titanium dioxide (TiO_2) nanoparticles embedded in the void surface. The beads exhibited high photocatalytic efficiency, up to 99.4 % methyl orange could be degraded in 2.5 h photocatalysis in the water containing the bead of 0.46 wt%. Moreover, stable cyclic usage in wastewater treatment was proved to be feasible, and not any decrease in the photocatalytic performance was found for the use in their later 9 cycles, which make the bead material an ideal and potential photocatalyst in wastewater industry.

Keywords High internal phase emulsion · Pickering emulsion · PolyHIPE · Porous beads · Photocatalyst

Introduction

Heterogeneous photocatalytic technology utilizing semiconductor catalysts has been considered to be efficient and promising in the wastewater industry because this advanced oxidation process can completely and rapidly mineralize a wide range of refractory organics to innocuous carbon dioxide and water [1–3]. However, most of these semiconductor catalysts are fine powders and applied in a suspension form, which entails complex post-separation of catalyst particles and possibly brings about the contamination of these catalyst solid in the treated water. Hence, various inorganic porous materials, such as zeolites [4], clays [5], activated carbon [6], and sepiolites [7, 8], have been employed to support photocatalysts. As for the disadvantages of these supports, photocatalysts are usually loaded onto the supports by physical adsorption which leads to relatively low loading content and slight catalytic particle leakage while using. Here, we present a novel macroporous support for photocatalysts: Pickering high internal phase emulsion (HIPE) templated poly(acrylamide/N, N′-methylene bisacrylamide) (P(AM/MBAM)) beads which are loaded with titanium dioxide (TiO_2) nanoparticles in the surface layer of the void walls. P(AM/MBAM) was chosen as polymer matrix due to its high hydrophilicity, which would make it easier for water to penetrate into the porous polymer beads.

HIPEs are often defined as the emulsions with dispersed phase more than 74 % of the emulsion volume [9–12]. And a macroporous material (polyHIPE) can be obtained by polymerizing the monomer in the continuous phase of HIPE and then removing the emulsion droplets [13–25]. These porous materials typically have low densities, high porosities and tunable void sizes ranging from 1 to 100 μm, which are ideal materials for catalyst supports [26]. As such, some metal nanoparticle catalysts, like gold [27] and palladium nanoparticles [28], have been immobilized onto the already produced polyHIPEs. But these synthesis processes involved a complicated two-step approach. Recently, inorganic particles [29–32], copolymer particles [33–36] and carbon nanotubes

Zhu holds a Ph.D, East China University of Science and Technology.
Hua holds a Ph.D, East China University of Science and Technology.
Zhang holds a Ph.D, East China University of Science and Technology.
Prof. Chen, East China University of Science and Technology.

✉ Shengmiao Zhang
shmzhang@ecust.edu.cn

✉ Jianding Chen
jiandingchen@ecust.edu.cn

[1] Shanghai Key Laboratory of Advanced Polymeric Materials, Key Laboratory for Ultrafine Materials of Ministry of Education, School of Materials Science and Engineering, East China University of Science and Technology, Shanghai 200237, China

[37] have been respectively substituted for traditional surfactant utilized in HIPE templates as stabilizers. In particle-stabilized HIPE (Pickering HIPE) template, particles would stand at the oil–water interface to prevent the coalescence of the adjacent droplets, and these stabilizer particles can thus be embedded in the surface layer of the polymer matrix (poly-Pickering-HIPE) after polymerization [38, 39]. In this study, the commercial TiO_2 nanoparticles (Degussa P25) were used as the stabilizer of the oil-in-water (O/W) Pickering HIPE template, which enables the loading of the photocatalyst TiO_2 nanoparticles to be achieved directly through the HIPE polymerization and impels the polymer matrix to clutch these photocatalyst nanoparticles to avoid the catalyst leakage in the later use.

Up to date, the most common physical form of a poly-Pickering-HIPE is a monolith [40]. Nevertheless, when they are applied as supports for photocatalyst, particulate poly-Pickering-HIPEs (i.e., porous beads) are preferred because they can get more photon penetration than monolith blocks. Therefore, the sedimentation polymerization method based on an oil-in-water-in-oil emulsion template, described by Zhang et al. [41, 42], Deleuze et al. [43] and Štefanec et al. [44] is utilized here to fabricate the poly-Pickering-HIPE beads. The obtained porous beads should be uniform and possess diameters greater than 1.0 mm, which can be easily separated from the media by filtration and recycled for further use.

Experimental section

Materials

Ammonium persulfate (APS, 98 %, Shanghai Lingfeng Chemical Reagent Co. Ltd) were recrystallised twice in deionised water before use. Acrylamide (AM, 98.5 %, Shanghai Lingfeng Chemical Reagent Co. Ltd), N, N′-methylene bisacrylamide (MBAM, 98 %, Sinopharm Chemical Reagent Co. Ltd), Tween 85 (Sinopharm Chemical Reagent Co. Ltd), paraffin liquid (Shanghai Lingfeng Chemical Reagent Co., Ltd), N, N, N, N-tetramethylethylenediamine (TMEDA, Shanghai Lingfeng Chemical Reagent Co., Ltd), titania nanoparticles (TiO_2, Degussa P25, average particle diameter: 21 nm), Methyl Orange (MO, Sinopharm Chemical Reagent Co. Ltd) and hydrochloric acid (HCl, 37 %, Shanghai Lingfeng Chemical Reagent Co. Ltd) were used as received. Water was freshly deionised.

Preparation of poly-Pickering-HIPE beads

TiO_2 nanoparticles were initially dispersed into 4 ml aqueous solution of surfactant Tween 85 (0.04 g, 1.0 wt%),. Then the monomer AM (1.420 g, 20 mmol), the crosslinker MBAM (0.309 g, 2 mmol) and the initiator APS (0.04 g, 1 wt%) were dissolved in the above TiO_2 nanoparticles dispersion. The solution obtained was used as aqueous phase. The Pickering HIPE was prepared by mixing aqueous phase with the paraffin (16 ml, as oil phase), and homogenising the mixture using an Ultra Turrax T18 homogeniser (7.5 mm rotor) operating at 14, 000 rpm for 3 min. The HIPE obtained was then dropped into a glass reaction column containing the paraffin with 2 % TMEDA(as catalyst to accelerate the polymerization) by using a syringe pump (Longer Pump LSP01-1A) at 50 °C. The O/W HIPE droplets were left in the sedimentation column at 50 °C to complete the polymerization. The polymerized beads were removed from the column, dried in a vacuum at 50 °C for 24 h, and extracted in Soxhlet apparatus with acetone to remove the paraffin. Finally, the resulting porous beads were dried to constant weight in a vacuum at 50 °C.

Photocatalysis of MO with the poly-Pickering-HIPEs

The photocatalytic degradation reaction using UV was carried out in a 25 ml glass vessel at room temperature (25 °C), being filled with 15 ml MO aqueous (20 ppm, PH=2 which was adjusted by hydrochloric acid) and 69 mg porous bead photocatalyst under constant oscillating. Six 10 W UV lamps with a maximum emission at 254 nm was positioned about 30 cm above the photo-reactor. After the reaction was completed, the porous beads were dredged out and then washed by water for further use, and the treated solution was collected. For a comparison of the efficiency of the bead systems, porous beads was replaced by 3.0 mg pure TiO_2 nanoparticles(not embedded in polymer beads). The mass of TiO_2 nanoparticles used was equal to that of the TiO_2 contained in 69 mg porous bead PB-2 which was prepared with 2.0 wt% TiO_2 in the aqueous phase(see Table 1).

Characterization

Photographs of the porous beads were taken utilizing a Canon S95 digital camera. The average bead diameter (d_b) was measured from the photographs directly. The TiO_2 nanoparticle content of the poly-Pickering-HIPEs was measured via a NETZSCH STA 449 F3 thermogravimetric analyzer (TGA) from room temperature to 800 °C at heating rates of 5 °C/min under air atmosphere. Five specimen were analyzed for each sample, and the TiO_2 content of the sample was given as the average value of these five specimen. Scanning electron microscope (SEM) images of Au-coated porous materials were taken with a Hitachi S-4800 SEM. The average void diameter (d_v) of the polyHIPEs was estimated from the SEM images. And at least 100 voids were measured for each sample. The average void diameter measured in this way is underestimates of the real values. Therefore it is necessary to introduce a statistical correction [43]. The average void diameter (d_v) of the polyHIPEs in this work was calculated by $d_v=2r/(3^{1/2})$,

Table 1 Composition of emulsion templates and the parameters of the resulting porous beads

Sample	$[TiO_2]$ / wt% [a]	d_b / mm [b]	d_v / μm [c]	d_i / μm [d]	I / % [e]	$[TiO_2]$ / wt% [f]
PB-1	1.0	2.3	22.6	6.7	16.0	2.20
PB-2	2.0	2.4	18.9	6.0	18.8	4.32
PB-4	4.0	2.5	10.8	4.3	29.6	8.14

[a] Feeding TiO_2 concentration respect to the water in aqueous phase

[b] The average bead diameters, calculated from the photographs

[c] The average void diameters inside the beads, calculated from SEM images

[d] The average interconnecting pore diameters inside the beads, calculated from SEM images

[e] Interconnectivity of the bead internal structure, calculated by $0.25n\times(d_i/d_v)^2\times100$, where n is the average number of interconnecting pores per void

[f] TiO_2 content in porous beads, determined by TGA

where r was the diameter value calculated from the SEM image. The average interconnecting pore diameter (d_i) was measured from the SEM images directly. And at least 100 interconnecting pores were measured for each sample. The interconnectivity (I) of the PolyHIPEs was calculated by $I=0.25n\times(d_i/d_v)$, where n was the average number of interconnecting pores per void and was also calculated from SEM images. At least 50 voids were calculated for each sample. In addition, the poly-Pickering-HIPEs were embedded in resin, cured and sliced into thick sections. These sections were then placed on a holey copper grid, and relevant TEM images were taken using the JEOL JEM 1400 TEM.

The concentration of MO in the solution before/after photocatalytic degradation was determined with a UV-2550PC UV–vis spectrophotometer by monitoring the absorbance values at 507 nm wavelength that was the maximum absorption wavelength of MO at PH=2.

Results and discussion

These produced poly-Pickering-HIPE materials were uniform and unagglomerated spherical beads (Fig. 1). As shown in Fig. 2, the bead materials possessed a typical polyHIPE morphology (i.e., a large number of voids were separated by polymer films), which was a skeletal replica of the O/W HIPE precursor. And it is imperative to note that both the external and the internal void structure of the polymer beads were highly interconnected. Specifically, these open voids on the bead surface, which were connected to the bead interior, not only can diminish the mass transfer limitations but may

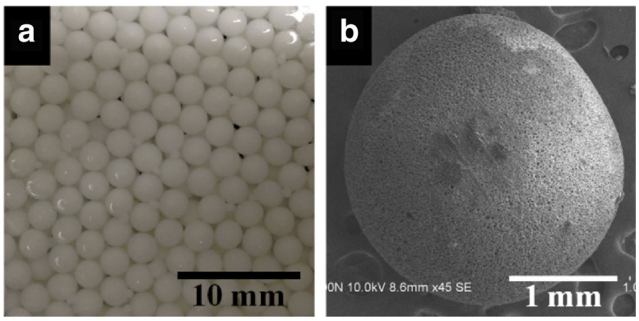

Fig. 1 Photograph (**a**) and SEM image (**b**) for poly-Pickering-HIPE beads (PB-2)

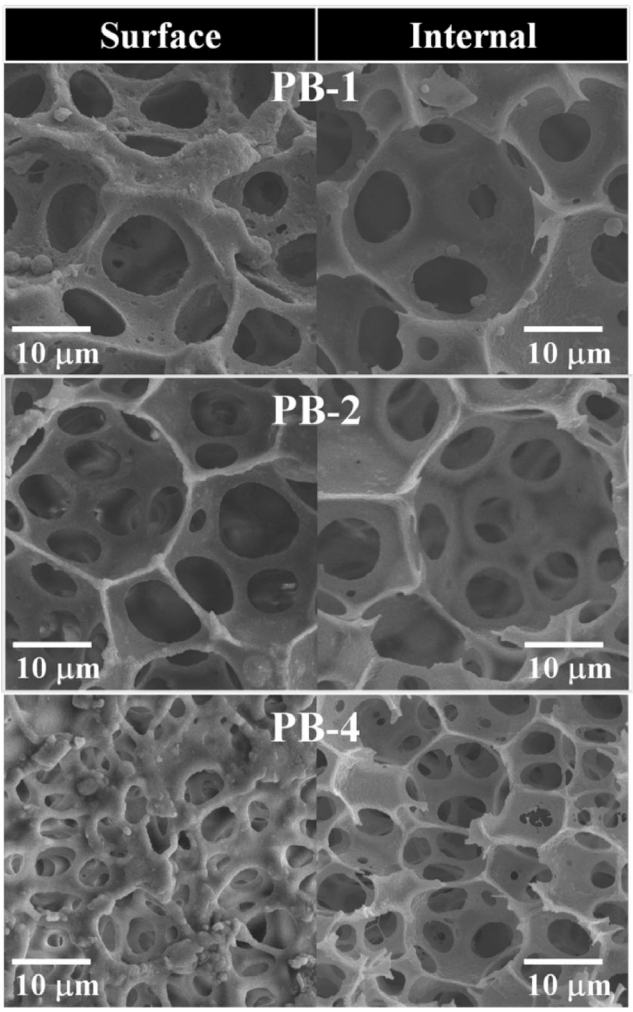

Fig. 2 SEM images for the surface and internal morphology of the poly-Pickering-HIPE beads with different TiO_2 nanoparticle concentration in the emulsion templates

increase the amount of photocatalyst active sites, when the beads are used as heterogeneous photocatalysts.

In attempt to explore the effect of TiO_2 on the morphology of poly-Pickering-HIPE beads and their efficiency of photocatalyst, HIPEs having feeding TiO_2 nanoparticle concentration of 1.0, 2.0, and 4.0 wt% were prepared, and resulting poly-Pickering-HIPEs (PB-1, PB-2 and PB-4) were obtained, respectively. TGA analysis of these beads showed that the final content of TiO_2 in PB-1, PB-2 and PB-4 were 2.20, 4.32 and 8.14 wt%, respectively.

Table 1 shows that the porous beads with different feeding TiO_2 nanoparticle concentration had similar bead sizes, while the void size and the interconnectivity of the poly-Pickering-HIPE beads could be tuned by changing the feeding TiO_2 nanoparticle concentration. The augment of TiO_2 nanoparticle concentration from 1.0 wt% to 2.0 and 4.0 wt% decreased the average void diameter of the polymer beads from 22.6 to 18.9 and 10.8 μm and raised the interconnectivity from 16.0 to 18.8 % and 29.6 %, respectively (Table 1). This is because increasing the amount of stabilizer TiO_2 nanoparticles would enhance the HIPE stability to coalescence, which led to relatively small average void diameter and high interconnectivity resulted from the thinner polymer films. However, it should be noticed that a high TiO_2 nanoparticle concentration (4.0 %) would render the bead surface more solid and less interconnected (Fig. 2).

As a photocatalyst support, the position of the photocatalyst TiO_2 nanoparticles in the bead is quite important. Here, TEM was used to observe and analyze the arrangement of TiO_2 nanoparticles. From the TEM images (Fig. 3a), it can be seen that a row of TiO_2 nanoparticles (black points) were located on the surface of the polymer walls, which benefit for the TiO_2 to be excited in later application. Since the produced porous polymers are a replica of the pore structure of the emulsion at the gel point [9, 10], the nanoparticle stabilizer of the emulsion template standing in the surface layer of void walls meant that the TiO_2 nanoparticles adsorbed in the water–oil interface and formed layers at the oil drop surface, which provided steric (mechanical) hindrance to droplet coalescence [44]. Moreover, the inner part of the polymer walls also contained some TiO_2 nanoparticles (Fig. 3b). This is attributed to both the good hydrophilicity of the particles and the presence of Tween85 in the emulsion. The hydrophilicity make the particles are able to disperse in aqueous phase well. Tween85 would adsorb on the oil–water interface competitively with TiO_2 nanoparticles [32]. And Tween85 could also adsorbs at the particle surface, thus changing its wetting properties, thereby disaggregating the particles, leaving them well dispersed in the aqueous phase [29].

Then, to evaluate the photocatalytic performance of these poly-Pickering-HIPE beads and their ability of treating industrial wastewater, photocatalytic oxidations of a MO dye, which was used as a pollutant model, were carried out at 25 °C by directly adding the porous beads into a MO aqueous (20 ppm) under constant oscillating with UV irradiation (λ= 254 nm). As shown in Fig. 4, the beads displayed great efficiency in degrading the MO dye, the red MO aqueous transformed to a colorless transparent solution after 2.5 h photocatalytic oxidation with the porous beads. In attempt to know the details of oxidation, the percentage of the MO removals from water after the reaction was determined by the change of the absorbance peak at 507 nm wavelength using a UV spectrophotometer. As shown in Fig. 5, at the beginning of the test, when porous beads was employed as photocatalyst, the oxidation rate of MO dye was slower than that in the test where pure TiO_2 nanoparticles were used. While after 2.5 h reaction, 99.2, 99.4 and 99.4 % of the MO dye was consumed, when PB-1, PB-2 and PB-4 were used as the photocatalysts, respectively, which were similar to the percentage (99.5 %) of MO dye removed by pure TiO_2 nanoparticles at the same time, and were much higher than the ratio (60.6 %) of MO molecules degraded under the circumstance of no catalyst.

Despite of the good photocatalytic effect, it is still worthy to note that there was not much difference in the photocatalytic performance among these polymer beads with different content of TiO_2 nanoparticles (Fig. 5).

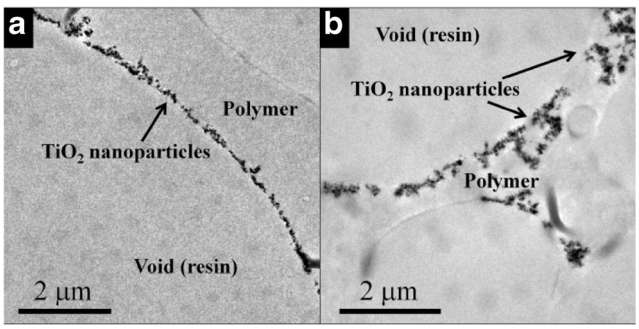

Fig. 3 TEM images for poly-Pickering-HIPE beads (PB-2) showing the exact location of the TiO_2 nanoparticles in the beads

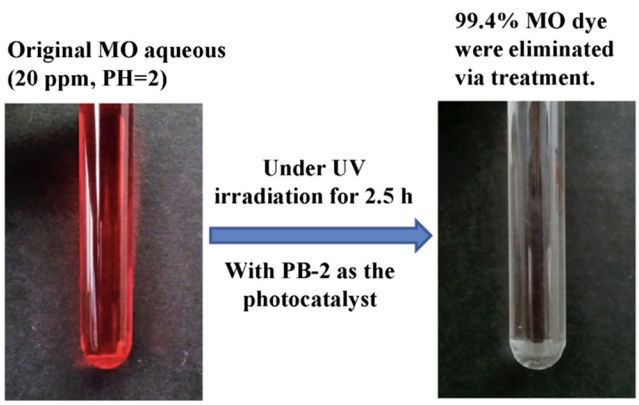

Fig. 4 The photocatalytic performance of the porous bead PB-2 for eliminating the MO dyes under UV irradiation for 2.5 h

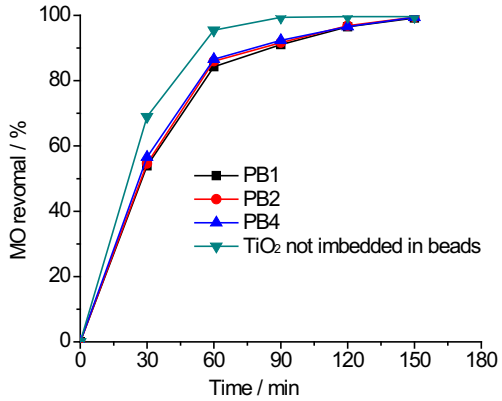

Fig. 5 The removal of the MO dyes from the water with poly-Pickering-HIPE beads or pure TiO_2 nanoparticles as the photocatalyst

This may be due to the fact that the voids and the interconnecting pores on the bead surface layer are still not large enough to achieve the UV ray penetration so that the TiO_2 nanoparticles inside the beads are difficult to be excited, and only the TiO_2 nanoparticles on the surface layer take effect. And due to part of the TiO_2 nanoparticles still remaining in the polymer matrix, the content of the TiO_2 nanoparticles on the bead surface that work indeed are almost similar, no matter how much TiO_2 nanoparticles existing inside the beads.

Another nine recycling experiments were also performed with PB-2 for photocatalytic oxidation of MO under UV irradiation. The percentage of MO removals in each cycle was monitored (Fig. 6). It is found that the amount of the degraded MO dye from the solution was always kept as high as 99 % for each run, indicating the cyclic usage of the porous beads is feasible and their stability in the wastewater is considerable satisfactory. All of these are thanks to the tight clutch of the TiO_2 nanoparticles by the polymer matrix via polymerization, which effectively avoids the leakage of these photocatalyst nanoparticles into the solution during their wastewater treatment.

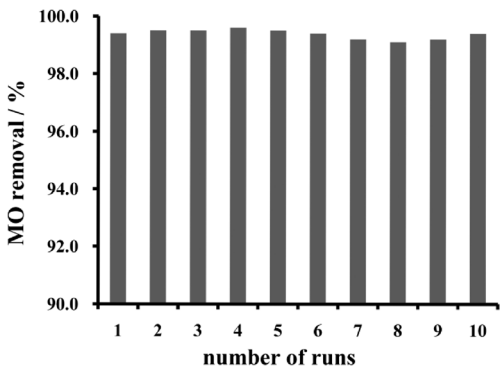

Fig. 6 Repeatedly employing a same batch of porous bead PB-2 as the photocatalyst to purify the MO dyes aqueous

Conclusions

In summary, a novel polymeric support for heterogeneous photocatalytic reactions was fabricated by using a multiple O/W/O emulsion as the template, which was an open-cell macroporous bead with photocatalyst TiO_2 nanoparticles embedded in the void surface. These poly-Pickering-HIPE beads showed their high photocatalytic efficiency in wastewater treatment. There were up to 99.4 % of the MO dye in water being consumed after 2.5 h reaction with the macroporous beads of 0.46 wt% in water, Moreover, their cyclic usage for purifying the wastewater was proved to be feasible and not any decrease in the photocatalytic performance was found for the use in their later cycle.

Acknowledgments This research was supported by the National Natural Scientific Foundation of China (51103042, 51203048), the Fundamental Research Funds for the Central Universities, Innovation Program of Shanghai Municipal Education Commission (12ZZ056), and Shanghai Key Laboratory Project (08DZ2230500).

References

1. Legrini O, Oliveros E, Braun AM (1993) Chem Rev 93:671–698
2. Fresno F, Portela R, Suárez S, Coronado JM (2014) J Mater Chem A 2:2863–2884
3. Miyauchi M, Nukui Y, Atarashi D, Sakai E (2013) ACS Appl Mater Interfaces 5:9770–9776
4. Guo P, Wang XS, Guo HC (2009) Appl Catal B 90:677–687
5. Li G, Zhao XS, Ray MB (2007) Sep Purif Technol 55:91–97
6. Jsmil TS, Ghaly MY, Fathy NA, Abd el-halim TA, Österlund L (2012) Sep Purif Technol 98:270–279
7. Aranda P, Kun R, Martin-Luengo MA, Letaief S, Dekany I, Ruiz-Hitzky E (2008) Chem Mater 20:84–91
8. Nieto-Suarez M, Palmisano G, Ferrer ML, Gutierrez MC, Yurdakal S, Augugliaro V, Pagliaro M, del Monte F (2009) J Mater Chem 19: 2070–2075
9. Kimmins SD, Cameron NR (2011) Adv Funct Mater 21:211–225
10. Cameron NR (2005) Polymer 46:1439–1449
11. Zhu Y, Zhang S, Hua Y, Zhang H, Chen J (2014) Ind Eng Chem Res 53:4642–4649
12. Pulko I, Krajnc P (2012) Macromol Rapid Commun 33:1731–1746
13. Silverstein MS (2014) Prog Polym Sci 39:199–234
14. Xu WF, Bai R, Zhang FA (2014) J Polym Res 21:524. doi:10.1007/s10965-014-0524-2
15. Zheng Z, Zheng X, Wang H, Du Q (2013) ACS Appl Mater Interfaces 5:7974–7982
16. Wang S, Zhang Z, Liu H, Zhang W, Qian Z, Wang B (2010) Colloid Polym Sci 288:1031–1039
17. Zhang S, Chen J (2007) Polymer 48:3021–3025
18. Zhang S, Chen J, Lykakis IN, Perchyonok VT (2010) Curr Org Synth 7:177–188
19. Lee KY, Blaker JJ, Murakami R, Heng JYY, Bismarck A (2014) Langmuir 30:452–460
20. Wong LLC, Barg S, Menner A, Pereira PV, Eda G, Chowalla M, Saiz E, Bismarck A (2014) Polymer 55:395–402
21. Liu W, He G, He Z (2012) J Polym Res 19:9765. doi:10.1007/s10965-011-9765-5
22. Zhu Y, Zhang S, Hua Y, Chen J, Hu CP (2010) Polymer 51:3612–3617

23. Hua Y, Chu Y, Zhang S, Zhu Y, Chen J (2013) Polymer 54:5852–5857
24. Kovačič S, Krajnc P, Slugovc C (2010) Chem Commun 46:7504–7506
25. Kovačič S, Štefanec D, Krajnc P (2007) Macromolecules 40:8056–8060
26. Pulko I, Wall J, Krajnc P, Cameron NR (2010) Chem Eur J 16: 2350–2354
27. Feral-Martin C, Birot M, Deleuze H, Desforges A, Backov R (2007) React Funct Polym 67:1072–1082
28. Desforges A, Backov R, Deleuze H, Mondain-Monval O (2005) Adv Funct Mater 15:1689–1695
29. Ikem VO, Menner A, Horozov TS, Bismarck A (2010) Adv Mater 22:3588–3592
30. Menner A, Ikem V, Salgueiro M, Shaffer MSP, Bismarck A (2007) Chem Commun 2007:4274–4276
31. Ikem VO, Menner A, Bismarck A (2008) Angew Chem Int Ed 47: 8277–8279
32. Hua Y, Zhang S, Zhu Y, Chu Y, Chen J (2013) J Polym Sci Part A: Polym Chem 51:2181–2187
33. Zhang S, Chen J (2009) Chem Commun 2009:2217–2219
34. Zhang S, Zhu Y, Hua Y, Jegat C, Chen J, Taha M (2011) Polymer 52:4881–4890
35. Li Z, Ming T, Wang J, Ngai T (2009) Angew Chem Int Ed 48: 8490–8493
36. Colver P, Bon SAF (2007) Chem Mater 19:1537–1539
37. Menner A, Verdejo R, Shaffer M, Bismarck A (2007) Langmuir 23: 2398–2403
38. Hua Y, Zhang S, Chen J, Zhu Y (2013) J Mater Chem A 1:13970–13977
39. Gurevitch I, Silverstein MS (2011) Macromolecules 44:3398–3409
40. Silverstein MS (2014) Polymer 55:304–320
41. Zhang H, Hardy GC, Rosseinsky MJ, Cooper AI (2003) Adv Mater 15:78–81
42. Desforges A, Arpontet M, Deleuze H, Mondain-Monval O (2002) React Funct Polym 53:183–192
43. Carnachan RJ, Bokhari M, Przyborski SA, Cameron NR (2006) Soft Matter 2:608–616
44. Binks BP, Kirkland M (2002) Phys Chem Chem Phys 4:3727–3733